Phase Space Distribution Near the Self-Excited Oscillation Threshold

Yuvaraj Dhayalan, Ilya Baskin, Keren Shlomi, and Eyal Buks
Department of Electrical Engineering, Technion, Haifa 32000, Israel
(Received 31 December 2013; published 28 May 2014)

We study the phase space distribution of an optomechanical cavity near the threshold of self-excited oscillation. A fully on-fiber optomechanical cavity is fabricated by patterning a suspended metallic mirror on the tip of the fiber. Optically induced self-excited oscillation of the suspended mirror is observed above a threshold value of the injected laser power. A theoretical analysis based on the Fokker-Planck equation evaluates the expected phase space distribution near threshold. A tomography technique is employed for extracting phase space distribution from the measured reflected optical power vs time in steady state. Comparison between theory and experimental results allows the extraction of the device parameters.

DOI: 10.1103/PhysRevLett.112.210403 PACS numbers: 03.65.Yz, 05.40.-a, 42.50.Pq

Optomechanical cavities are currently a subject of intense basic and applied study [1–7]. Optomechanical cavities can be employed in various sensing [8–11] and photonics applications [12–18]. Moreover, such systems may allow experimental study of the crossover from classical to quantum mechanics [2,19–27] (see Ref. [28] for a recent review). When the finesse of the optical cavity that is employed for constructing the optomechanical cavity is sufficiently high, the coupling to the mechanical resonator that serves as a vibrating mirror is typically dominated by the effect of radiation pressure [2,5,29–32]. On the other hand, bolometric effects can contribute to the optomechanical coupling when optical absorption by the vibrating mirror is significant [7,33–40]. In general, bolometric effects play an important role in relatively large mirrors, in which the thermal relaxation rate is comparable to the mechanical resonance frequency [36,38,41,42]. Phenomena such as mode cooling and self-excited oscillation [3,20,36,37,41,43–45] have been shown in systems in which bolometric effects are dominant [7,33,37,41,49,50].

Recently, it has been demonstrated that optomechanical cavities can be fabricated on the tip of an optical fiber [46,47,51–57]. These miniature devices appear to be very promising for sensing applications. However, their operation requires external driving of the on-fiber mechanical resonator. Traditional driving using either electrical or magnetic actuation, however, is hard to implement with a mechanical resonator on the tip of an optical fiber, a limitation that can be overcome by optical actuation schemes [48].

In this Letter, we study a configuration of an on-fiber optomechanical cavity and demonstrate that self-excited oscillation can be optically induced by injecting a monochromatic laser light into the fiber. The optomechanical cavity is formed between the vibrating mirror that is fabricated on the tip of a single mode optical fiber and an additional static reflector. The results seen in Figs. 1 and 2 below have been obtained with a sample (labeled as sample *A*) in which the static reflector is the glass-vacuum interface at the fiber's tip, whereas the results seen in Fig. 3 have been obtained with a sample (labeled as sample *B*) in which the static reflector is a fiber Bragg grating (FBG). For both samples, optically induced self-excited oscillation is attributed to the bolometric optomechanical coupling between the optical mode and the mechanical resonator [49,50].

Optomechanical cavities operating in the region of self-excited oscillation can be employed for sensing applications. Such a device can sense physical parameters that affect the mechanical properties of the suspended mirror

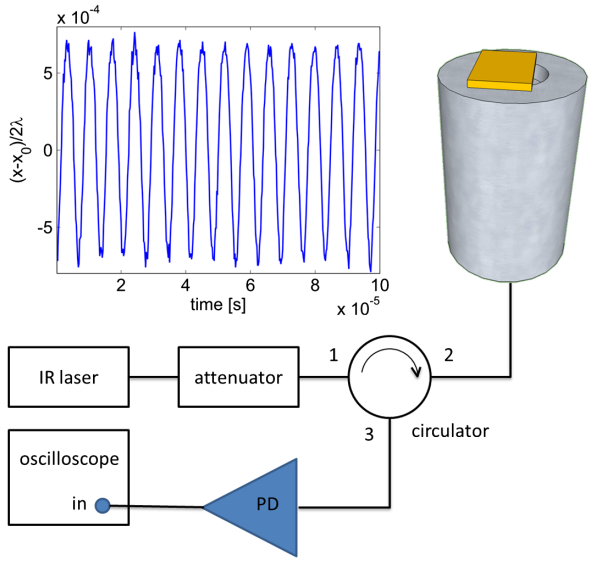

FIG. 1 (color online). A schematic drawing of sample *A* and the experimental setup. An on-fiber optomechanical cavity is excited by a laser. The reflected light intensity is measured and analyzed. The inset shows a typical trace of the normalized displacement $(x - x_0)/\lambda$ vs time measured by the oscilloscope above the self-excited oscillation threshold with $\Delta P_L/P_{\mathrm{LC}} = 0.034$. The photodetector signal is translated to displacement by measuring the thermomechanical noise and employing the calibration method that is described in Ref. [58].

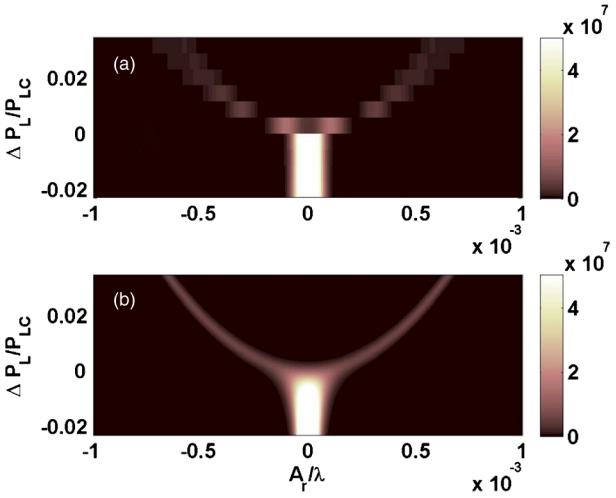

FIG. 2 (color online). The dependence on laser power P_L for sample A. (a) Phase space distribution extracted from the measured probability distribution function $w(X'_\phi)$ using Eq. (6). (b) Phase space distribution calculated using Eq. (5). The following device parameters have been employed for generating the plot in panel (b): $\omega_0 = 2\pi \times 144$ kHz, $\lambda = 1.55$ μm, $T_{\text{eff}} = 300$ K, $s_D = 0.8$, and $\gamma_2\lambda^2/\gamma_0 = 8 \times 10^4$.

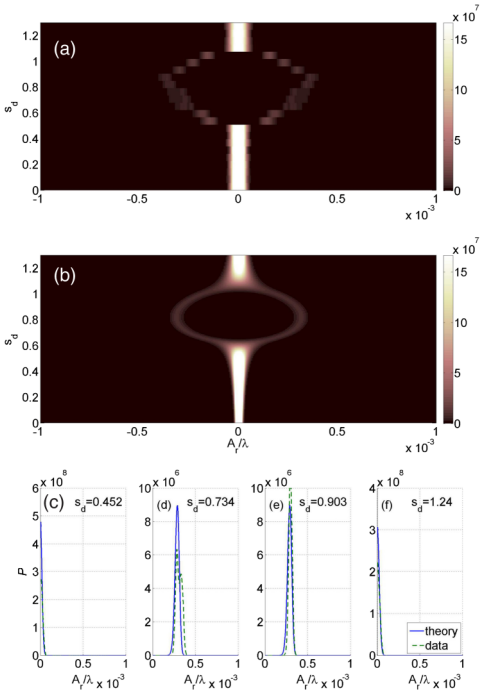

FIG. 3 (color online). The dependence on wavelength λ for sample B. The static mirror of the optomechanical cavity is provided by a fiber Bragg grating mirror (made using a standard phase mask technique [59], grating period of 0.527 μm and length ≈8 mm) with the reflectivity band of 0.4 nm full width at half maximum centered at 1550 nm. The length of the optical cavity was 10 mm. (a) Phase space distribution extracted from the measured probability distribution function $w(X'_\phi)$ using Eq. (6). The laser wavelength is varied from the cavity resonance value of $\lambda_R = 1.545135$ μm, for which the detuning factor s_D vanishes, to 1.545158 μm, for which $s_D = 1.3$. (b) Phase space distribution calculated using Eq. (5). The following device parameters have been employed for generating the plot in panel (b): $\omega_0 = 2\pi \times 225$ kHz, $m = 1.1 \times 10^{-12}$ kg, $\beta_+ = 0.68$, $T_{\text{eff}} = 300$ K, and $\gamma_2\lambda^2/\gamma_0 = 5 \times 10^5$. Panels (c)–(f) show cross sections of the top color maps at different values of the detuning factor s_D.

(e.g., absorbed mass, heating by external radiation, acceleration, etc.). The sensitivity of such a sensor is limited by the phase noise of the self-excited oscillation. Here, we experimentally measure the phase space distribution of the mechanical element near the threshold of self-excited oscillation and compare the results with theoretical predictions.

The optomechanical cavity schematically shown in Fig. 1 was fabricated on the flat polished tip of a single mode fused silica optical fiber having outer diameter of 126 μm (Corning SMF-28 operating at wavelength band around $\lambda = 1550$ nm) held in a zirconia ferrule. Thermal evaporation through a mechanical mask was employed for patterning a metallic rectangle (see Fig. 1) made of a 10 nm thick chromium layer and a 200 nm thick gold layer. The metallic rectangle, which serves as a mirror, covers almost the entire fiber cross section. However, a small segment is left open in order to allow suspension of the mirror, which was done by etching approximately 12 μm of the underlying silica in 7% HF acid (90 min etch time at room temperature). The suspended mirror remained supported by the zirconia ferrule, which is resistant to HF.

Monochromatic light was injected into the fiber of sample A from a laser source having wavelength $\lambda = 1550.08$ nm and an adjustable power level P_L. The laser was connected through an optical circulator that allowed the measurement of the reflected light intensity (P_R) by a fast responding photodetector. The detected signal was analyzed by an oscilloscope and a spectrum analyzer (see Fig. 1). The experiments were performed in vacuum (at residual pressure below 0.01 Pa). The angular frequency of the fundamental mode of the suspended mirror $\omega_0 = 2\pi \times 144$ kHz was estimated by the frequency of thermal oscillation measured at low input laser power. When the injected laser power P_L exceeds a threshold value given by $P_{\text{LC}} = 4.3$ mW, optically induced self-excited oscillation of the vibrating mirror is observed (see Fig. 1).

In the limit of small displacement, the dynamics of the system can be approximately described using a single evolution equation [49]. The theoretical model that is used to derive the evolution equation is briefly described below. Note that some optomechanical effects that were taken into account in the theoretical modeling [49] were found experimentally to have a negligible effect on the dynamics [50] (e.g., the effect of radiation pressure). In what follows, such effects are disregarded.

The micromechanical mirror in the optical cavity is treated as a mechanical resonator with a single degree of

freedom x having mass m and linear damping rate γ_0 (when it is decoupled from the optical cavity). It is assumed that the angular resonance frequency ω_m of the mechanical resonator depends on the temperature T of the suspended mirror. For small deviation of T from the base temperature T_0 (i.e., the temperature of the supporting substrate) ω_m is taken to be given by $\omega_m = \omega_0 - \beta(T - T_0)$, where β is a constant. Furthermore, to model the effect of thermal deformation [37] it is assumed that a temperature-dependent force given by $F_{\rm th} = \theta(T - T_0)$, where θ is a constant, acts on the mechanical resonator [40].

The intracavity optical power incident on the suspended mirror, which is denoted by $P_L I(x)$, where P_L is the injected laser power, depends on the mechanical displacement x (i.e., on the length of the optical cavity). For small x, the expansion $I(x) \simeq I_0 + I_0' x + (1/2) I_0'' x^2$ is employed, where a prime denotes differentiation with respect to the displacement x. The time evolution of the effective temperature T is governed by the thermal balance equation $\dot{T} = \kappa(T_0 - T) + \eta P_L I(x)$, where overdot denotes differentiation with respect to time t, η is the heating coefficient due to optical absorption, and κ is the thermal decay rate.

The function $I(x)$ depends on the properties of the optical cavity formed between the suspended mechanical mirror and the on-fiber static reflector (the glass-vacuum interface on the fiber's tip for sample A or FBG for sample B). The finesse of the optical cavity is limited by loss mechanisms that give rise to optical energy leaking out of the cavity. The main escape routes are through the on-fiber static reflector, through absorption by the metallic mirror, and through radiation. The corresponding transmission probabilities are respectively denoted by T_B, T_A, and T_R. In terms of these parameters, the function $I(x)$ is given by [50]

$$I(x) = \frac{\beta_F (1 - (\beta_-^2/\beta_+^2))\beta_+^2}{1 - \cos(4\pi x_D/\lambda) + \beta_+^2}, \tag{1}$$

where $x_D = x - x_R$ is the displacement of the mirror relative to a point x_R, at which the energy stored in the optical cavity in steady state obtains a local maximum, $\beta_\pm^2 = (T_B \pm T_A \pm T_R)^2/8$ and where β_F is the cavity finesse. The reflection probability $R_C = P_R/P_L$ is given in steady state by [50,60] $R_C = 1 - I(x)/\beta_F$.

The displacement $x(t)$ can be expressed in terms of the complex amplitude A as $x(t) = x_0 + 2{\rm Re}A$, where x_0, which is given by $x_0 = \eta\theta P_L I_0/\kappa\omega_0^2$, is the optically induced static displacement. For a small displacement, the evolution equation for the complex amplitude A is found to be given by [49]

$$\dot{A} + (\Gamma_{\rm eff} + i\Omega_{\rm eff})A = \xi(t), \tag{2}$$

where both the effective resonance frequency $\Omega_{\rm eff}$ and the effective damping rate $\Gamma_{\rm eff}$ are real even functions of $|A|$. To second order in $|A|$ they are given by

$$\Gamma_{\rm eff} = \Gamma_0 + \Gamma_2 |A|^2, \qquad \Omega_{\rm eff} = \Omega_0 + \Omega_2 |A|^2, \tag{3}$$

where $\Gamma_0 = \gamma_0 + \eta\theta P_L I_0'/2\omega_0^2$, $\Gamma_2 = \gamma_2 + \eta\beta P_L I_0''/4\omega_0$, γ_2 is the mechanical nonlinear quadratic damping rate [61], $\Omega_0 = \omega_0 - \eta\beta P_L I_0/\kappa$, and $\Omega_2 = -\eta\beta P_L I_0''/\kappa$. Note that the above expressions for $\Gamma_{\rm eff}$ and $\Omega_{\rm eff}$ are obtained by making the following assumptions: $\beta x_0 \ll \theta/2\omega_0$, $\theta\kappa^2 \ll \beta\omega_0^3\lambda$, where λ is the optical wavelength, and $\kappa \ll \omega_0$, all of which typically hold experimentally [50]. The fluctuating term [62] $\xi(t) = \xi_x(t) + i\xi_y(t)$, where both ξ_x and ξ_y are real, represents white noise and the following is assumed to hold: $\langle \xi_x(t)\xi_x(t')\rangle = \langle \xi_y(t)\xi_y(t')\rangle = 2\Theta\delta(t-t')$ and $\langle \xi_x(t)\xi_y(t')\rangle = 0$, where $\Theta = \gamma_0 k_B T_{\rm eff}/4m\omega_0^2$, k_B is Boltzmann's constant, and $T_{\rm eff}$ is the effective noise temperature. Dependence of $T_{\rm eff}$ on mechanical amplitude $|A|$ due to nonlinear damping [see Eq. (42) of Ref. [63]] is disregarded since both γ_2 and $|A|$ are assumed to be small. In cylindrical coordinates, A is expressed as $A = A_r e^{iA_\theta}$, where $A_r = |A_r|$ and A_θ is real [64]. The Langevin equation for the radial coordinate A_r can be written as

$$\dot{A}_r + \frac{\partial \mathcal{H}}{\partial A_r} = \xi_r(t), \tag{4}$$

where $\mathcal{H}(A_r) = \Gamma_0 A_r^2/2 + \Gamma_2 A_r^4/4$ and the white-noise term $\xi_r(t)$ satisfies $\langle \xi_r(t)\xi_r(t')\rangle = 2\Theta\delta(t-t')$.

Consider the case where $\Gamma_2 > 0$, for which a supercritical Hopf bifurcation occurs when the linear damping coefficient Γ_0 vanishes. Above threshold, i.e., when Γ_0 becomes negative, Eq. (4) has a steady-state solution (when noise is disregarded) at the point $r_0 = \sqrt{-\Gamma_0/\Gamma_2}$ [see Eq. (3)]. The Langevin Eq. (4) yields a corresponding Fokker-Planck equation, which in turn can be used to evaluate the normalized phase space probability distribution function in steady state [62,64], which is found to be given by

$$\mathcal{P} = \frac{e^{-(A_r/\delta_0)^2 - (1/4\nu^2)(A_r/\delta_0)^4}}{\pi^{3/2}\delta_0^2 \nu e^{\nu^2}(1 - {\rm erf}\nu)}, \tag{5}$$

where $\delta_0^2 = 2\Theta/\Gamma_0$ and where $\nu = \Gamma_0/\sqrt{4\Gamma_2\Theta}$. Note that $\mathcal{P}$ is independent of the angle A_θ.

Experimentally, the technique of state tomography can be employed for extracting phase space probability distribution from measured displacement of the mechanical resonator. The normalized homodyne observable X_ϕ with a real phase ϕ is defined by $X_\phi = 2^{-1/2}(A^* e^{i\phi} + A e^{-i\phi})$. Let $w(X_\phi')$ be the probability distribution function of the observable X_ϕ. In general, with the help of the inverse Radon transform, the phase space probability distribution function $\mathcal{P}$ can be expressed in terms of the probability distribution functions $w(X_\phi')$ [65]. With a cw laser excitation, in steady state, $w(X_\phi')$ is expected to be ϕ independent. For such a case one finds that

$$\mathcal{P} = \frac{1}{2\pi}\int_0^\infty d\zeta \tilde{w}(\zeta)\zeta J_0(\zeta\sqrt{A_x^2 + A_y^2}), \tag{6}$$

where the notation J_n is used to label Bessel functions of the first kind, and where $\tilde{w}(\zeta)$, which is given by $\tilde{w}(\zeta) = \int_{-\infty}^{\infty} dX'_\phi w(X'_\phi) e^{-i\zeta X'_\phi}$, is the characteristic function of $w(X'_\phi)$; i.e., $\mathcal{P}$ is found to be the Hankel transform of the characteristic function $\tilde{w}(\zeta)$.

Sample A, which is seen schematically in Fig. 1, was used to study the dependence of phase space distribution on laser power. To that end, the photodetector signal (see Fig. 1) was recorded over a time period of 2 ms for different values of $\Delta P_L = P_L - P_{\mathrm{LC}}$, where P_L is the laser power and P_{LC} is the threshold value. Equation (6) together with the measured probability distribution function $w(X'_\phi)$ are employed to evaluate the phase space distribution seen in Fig. 2(a). Figure 2(b) exhibits the theoretical prediction for the phase space distribution based on Eq. (5). The device parameters that have been employed for generating the plot in Fig. 2(b) are listed in the caption of Fig. 2.

In another on-fiber optomechanical cavity (sample B) having a FBG mirror [50], the dependence on laser wavelength was investigated. The optical cavity in this device is significantly longer (in comparison with sample A), and consequently, larger cavity detuning can be achieved for a given change in optical wavelength. The experimental results are compared with theory in Fig. 3. The device parameters that have been employed for generating the plot in Fig. 3(b) are listed in the caption of Fig. 3. The results are presented as a function of the detuning dimensionless factor $s_D \equiv 4\pi x_D/\lambda\beta_+$, which is proportional to the detuning and inversely proportional to the resonance linewidth. For example, when cavity asymmetry is disregarded (i.e., when $\beta_- = 0$) and when $\beta_+ \ll 1$, the reflectivity obtains its half-maximum value $R_C = 0.5$ when $s_D = \sqrt{2}$. Note that positive values of s_D correspond to "red" detuning, i.e., $\lambda > \lambda_R = 1.545135\ \mu$m, where λ_R is the cavity resonance wavelength (see caption of Fig. 3).

In summary, tomography is employed to measure phase space distribution near the threshold of self-excited oscillation. The comparison with theory, which yields a good agreement, allows the extraction of device parameters, which in turn can be used to evaluate the expected sensitivity of sensors operating in the region of self-excited oscillation [8–11]. Even though self-excited oscillations can be optically driven in an on-fiber optomechanical cavity even without adding an FBG (as is demonstrated with sample A), a better control over cavity detuning and cavity finesse can be achieved when FBG is integrated (sample B).

This work was supported by the Israel Science Foundation, the Binational Science Foundation, the Deborah Foundation, the Robert J. Shillman Foundation, the Mitchel Foundation, the Israel Ministry of Science, the Russell Berrie Nanotechnology Institute, the European STREP QNEMS Project, MAGNET Metro 450 consortium, and MAFAT.

[1] V. B. Braginsky and A. B. Manukin, J. Exp. Theor. Phys. **52**, 986 (1967).
[2] S. Gigan, H. R. Böhm, M. Paternostro, F. Blaser, J. B. Hertzberg, K. C. Schwab, D. Bauerle, M. Aspelmeyer, and A. Zeilinger, Nature (London) **444**, 67 (2006).
[3] K. Hane and K. Suzuki, Sens. Actuators, A **51**, 179 (1995).
[4] I. Favero, C. Metzger, S. Camerer, D. Konig, H. Lorenz, J. P. Kotthaus, and K. Karrai, Appl. Phys. Lett. **90**, 104101 (2007).
[5] T. J. Kippenberg and K. J. Vahala, Science **321**, 1172 (2008).
[6] F. Marquardt and S. M. Girvin, Physics **2**, 40 (2009).
[7] C. H. Metzger and K. Karrai, Nature (London) **432**, 1002 (2004).
[8] O. Arcizet, P.-F. Cohadon, T. Briant, M. Pinard, A. Heidmann, J.-M. Mackowski, C. Michel, L. Pinard, O. Franais, and L. Rousseau, Phys. Rev. Lett. **97**, 133601 (2006).
[9] S. Forstner, S. Prams, J. Knittel, E. D. van Ooijen, J. D. Swaim, G. I. Harris, A. Szorkovszky, W. P. Bowen, and H. Rubinsztein-Dunlop, Phys. Rev. Lett. **108**, 120801 (2012).
[10] D. Rugar, H. J. Mamin, and P. Guethner, Appl. Phys. Lett. **55**, 2588 (1989).
[11] S. Stapfner, L. Ost, D. Hunger, J. Reichel, I. Favero, and E. M. Weig, Appl. Phys. Lett. **102**, 151910 (2013).
[12] G. Bahl, J. Zehnpfennig, M. Tomes, and T. Carmon, Nat. Commun. **2**, 403 (2011).
[13] M. Eichenfield, C. P. Michael, R. Perahia, and O. Painter, Nat. Photonics **1**, 416 (2007).
[14] N. Flowers-Jacobs, S. Hoch, J. Sankey, A. Kashkanova, A. Jayich, C. Deutsch, J. Reichel, and J. Harris, Appl. Phys. Lett. **101**, 221109 (2012).
[15] M. Hossein-Zadeh and K. J. Vahala, IEEE J. Sel. Top. Quantum Electron. **16**, 276 (2010).
[16] S. E. Lyshevski and M. A. Lyshevski, in *Third IEEE Conference on Nanotechnology, 2003* (IEEE, New York, 2003), Vol. 2, p. 840.
[17] N. Stokes, F. Fatah, and S. Venkatesh, Electron. Lett. **24**, 777 (1988).
[18] M. C. Wu, O. Solgaard, and J. E. Ford, J. Lightwave Technol. **24**, 4433 (2006).
[19] O. Arcizet, P.-F. Cohadon, T. Briant, M. Pinard, and A. Heidmann, Nature (London) **444**, 71 (2006).
[20] T. Carmon, H. Rokhsari, L. Yang, T. J. Kippenberg, and K. J. Vahala, Phys. Rev. Lett. **94**, 223902 (2005).
[21] C. Genes, D. Vitali, P. Tombesi, S. Gigan, and M. Aspelmeyer, Phys. Rev. A **77**, 033804 (2008).
[22] A. M. Jayich, J. C. Sankey, B. M. Zwickl, C. Yang, J. D. Thompson, S. M. Girvin, A. A. Clerk, F. Marquardt, and J. G. E. Harris, New J. Phys. **10**, 095008 (2008).
[23] H. J. Kimble, Y. Levin, A. B. Matsko, K. S. Thorne, and S. P. Vyatchanin, Phys. Rev. D **65**, 022002 (2001).
[24] P. Meystre, Ann. Phys. (Amsterdam) **525**, 215 (2013).
[25] A. Schliesser, R. Riviere, G. Anetsberger, O. Arcizet, and T. J. Kippenberg, Nat. Phys. **4**, 415 (2008).
[26] J. D. Teufel, D. Li, M. S. Allman, K. Cicak, A. J. Sirois, J. D. Whittaker, and R. W. Simmonds, Nature (London) **471**, 204 (2011).
[27] J. Thompson, B. Zwickl, A. Jayich, F. Marquardt, S. Girvin, and J. Harris, Nature (London) **452**, 72 (2008).
[28] M. Poot and H. S. van der Zant, Phys. Rep. **511**, 273 (2012).

[29] O. Arcizet, P. F. Cohadon, T. Briant, M. Pinard, and A. Heidmann, Nature (London) **444**, 71 (2006).
[30] T. J. Kippenberg, H. Rokhsari, T. Carmon, A. Scherer, and K. J. Vahala, Phys. Rev. Lett. **95**, 033901 (2005).
[31] D. Kleckner and D. Bouwmeester, Nature (London) **444**, 75 (2006).
[32] H. Rokhsari, T. Kippenberg, T. Carmon, and K. Vahala, Opt. Express **13**, 5293 (2005).
[33] G. Jourdan, F. Comin, and J. Chevrier, Phys. Rev. Lett. **101**, 133904 (2008).
[34] S. D. Liberato, N. Lambert, and F. Nori, Phys. Rev. A **83**, 033809 (2011).
[35] F. Marino and F. Marin, Phys. Rev. E **83**, 015202 (2011).
[36] F. Marquardt, J. G. E. Harris, and S. M. Girvin, Phys. Rev. Lett. **96**, 103901 (2006).
[37] C. Metzger, M. Ludwig, C. Neuenhahn, A. Ortlieb, I. Favero, K. Karrai, and F. Marquardt, Phys. Rev. Lett. **101**, 133903 (2008).
[38] M. Paternostro, S. Gigan, M. S. Kim, F. Blaser, H. R. Böhm, and M. Aspelmeyer, New J. Phys. **8**, 107 (2006).
[39] J. Restrepo, J. Gabelli, C. Ciuti, and I. Favero, C.R. Acad. Sci., Ser. IIb **12**, 860 (2011).
[40] D. Yuvaraj, M. B. Kadam, O. Shtempluck, and E. Buks, J. Microelectromech. Syst. **22**, 430 (2013).
[41] K. Aubin, M. Zalalutdinov, T. Alan, R. Reichenbach, R. Rand, A. Zehnder, J. Parpia, and H. Craighead, J. Microelectromech. Syst. **13**, 1018 (2004).
[42] S. De Liberato, N. Lambert, and F. Nori, Phys. Rev. A **83**, 033809 (2011).
[43] T. Carmon and K. J. Vahala, Phys. Rev. Lett. **98**, 123901 (2007).
[44] T. Corbitt, D. Ottaway, E. Innerhofer, J. Pelc, and N. Mavalvala, Phys. Rev. A **74**, 21802 (2006).
[45] K. Kim and S. Lee, J. Appl. Phys. **91**, 4715 (2002).
[46] C. Ma and A. Wang, Opt. Lett. **35**, 2043 (2010).
[47] A. B. Shkarin, N. E. Flowers-Jacobs, S. W. Hoch, A. D. Kashkanova, C. Deutsch, J. Reichel, and J. G. E. Harris, Phys. Rev. Lett. **112**, 013602 (2014).
[48] G. Gruca, D. Chavan, J. Rector, K. Heeck, and D. Iannuzzi, Sens. Actuators, A **190**, 77 (2013).
[49] S Zaitsev, O. Gottlieb, and E. Buks, Nonlinear Dynamics **69**, 1589 (2012).
[50] S. Zaitsev, A. K. Pandey, O. Shtempluck, and E. Buks, Phys. Rev. E **84**, 046605 (2011).
[51] F. Albri, J. Li, R. R. J. Maier, W. N. MacPherson, and D. P. Hand, J. Micromech. Microeng. **23**, 045021 (2013).
[52] I. Baskin, D. Yuvaraj, G. Bachar, K. Shlomi, O. Shtempluck, and E. Buks, arXiv:1210.7327 [J. Microelectromech. Syst. (to be published)].
[53] A. Butsch, M. S. Kang, T. G. Euser, J. R. Koehler, S. Rammler, R. Keding, and P. S. Russell, Phys. Rev. Lett. **109**, 183904 (2012).
[54] D. Chavan, G. Gruca, S. de Man, M. Slaman, J. H. Rector, K. Heeck, and D. Iannuzzi, Rev. Sci. Instrum. **81**, 123702 (2010).
[55] K. B. Gavan, J. H. Rector, K. Heeck, D. Chavan, G. Gruca, T. H. Oosterkamp, and D. Iannuzzi, Opt. Lett. **36**, 2898 (2011).
[56] D. Iannuzzi, S. Deladi, V. J. Gadgil, R. G. P. Sanders, H. Schreuders, and M. C. Elwenspoek, Appl. Phys. Lett. **88**, 053501 (2006).
[57] I. W. Jung, B. Park, J. Provine, R. Howe, and O. Solgaard, J. Lightwave Technol. **29**, 1367 (2011).
[58] E. Buks and M. L. Roukes, Phys. Rev. B **63**, 33402 (2001).
[59] D. Anderson, V. Mizrahi, T. Erdogan, and A. White, Electron. Lett. **29**, 566 (1993).
[60] B Yurke and E. Buks, J. Lightwave Technol. **24**, 5054 (2006).
[61] S. Zaitsev, O. Shtempluck, E. Buks, and O. Gottlieb, Nonlinear Dynamics **67**, 859 (2012).
[62] H. Risken, *The Fokker-Planck Equation: Methods of Solution and Applications* (Springer, New York, 1996).
[63] E. Buks, C.R. Phys. **13**, 454 (2012).
[64] R. D. Hempstead and M. Lax, Phys. Rev. **161**, 350 (1967).
[65] K. Vogel and H. Risken, Phys. Rev. A **40**, 2847 (1989).